J. Fluid Mech. (1985), *vol.* 154, *pp.* 145–162
Printed in Great Britain

Stokes wall effects for particles moving near cylindrical boundaries

By A. FALADE
Department of Mechanical Engineering, University of Lagos, Lagos, Nigeria

AND H. BRENNER
Department of Chemical Engineering, Massachusetts Institute of Technology, Cambridge, MA 02139

(Received 6 February 1984 and in revised form 30 July 1984)

An asymptotic scheme is derived for calculating values of the 'reflected' Stokeslet-field velocity dyadic $\boldsymbol{V}$ and its gradient $\nabla\boldsymbol{V}$ back at the Stokeslet location for situations in which this singular point lies in close proximity to the wall of an infinitely long circular cylinder. The asymptotic formulas furnished by this scheme permit calculations of first- and second-order wall effects in the non-dimensional parameter $\kappa = a/R_0$ ($a \equiv$ characteristic particle radius, $R_0 \equiv$ cylinder radius) upon the Stokes resistance of a particle of arbitrary shape, location and orientation when translating and/or rotating near the wall of an otherwise quiescent fluid-filled or fluid-surrounded circular cylinder. This reflection-type calculation is applicable for circumstances in which the inequalities $\kappa \ll 1$ and $1-\beta \ll 1$ are each separately satisfied, while simultaneously $\kappa/(1-\beta) \ll 1$. (Here $\beta = b/R_0$ is the fractionally eccentric Stokeslet location, or equivalently the centre of reaction of the particle, with b its distance from the tube axis.) The main result of this paper is the development of the pair of asymptotic wall-correction formulas

$$W_{jk} \sim {}_0C_{jk}(1-\beta)^{-1} + {}_1C_{jk} + {}_2C_{jk}(1-\beta) + O(1-\beta)^2$$

and

$$W_{jk,l} \sim {}_0D_{jkl}(1-\beta)^{-2} + {}_1D_{jkl}(1-\beta)^{-1} + {}_2D_{jkl} + O(1-\beta)$$

to particle resistance, with $\boldsymbol{W} \equiv W_{jk}$ and $\nabla\boldsymbol{W} \equiv W_{kl,j}$ respectively the non-dimensional normalized wall-effect dyadic and its gradient at the Stokeslet location β. The numerical, rational fraction, β-independent, ${}_nC_{jk}$ and ${}_nD_{jkl}$ coefficients ($n = 0, 1, 2$) appearing above are evaluated by solving a recursive sequence of Stokes-flow boundary-value problems in the semi-infinite fluid domain bounded by a plane wall. These simple asymptotic formulas are shown to agree excellently in the range near $\beta = 1$ with existing values derived from the exact solution of the original circular-cylinder boundary-value problem, involving tedious infinite-series summations of complicated Bessel-function integrands extended over infinite integration domains. Generalizations of the scheme to particle motion in the space *external* to a circular cylinder is briefly sketched, as too is the case of cylinders of non-circular cross-section.

1. Introduction

Cox & Brenner (1967) demonstrated that the hydrodynamic force $\boldsymbol{F}$ and torque $\boldsymbol{G}_0$ (about some arbitrary point O fixed in the particle) exerted on a particle moving in proximity to a wall bounding an otherwise quiescent Stokes flow may be expressed correctly to any order in κ by a sum of tensor products of various members of sets

of respective material particle and wall tensors, scalarly multiplied by the translational and angular velocities $\boldsymbol{U}_0$ and $\boldsymbol{\Omega}$ of the particle. For a prescribed particle, the material *particle* tensors (which are constant relative to body-fixed axes locked into the particle) depend solely upon the particle's geometric properties – namely its size a and shape, as well as upon the explicit location of O within the particle. Likewise, the material *wall* tensors (which are constant relative to space-fixed axes fixed in the tube walls) depend solely upon the tube radius R_0 and the lateral distance b of O from the tube axis.

Hirschfeld, Brenner & Falade (1984) demonstrated that the material wall tensors required to derive all terms in the expansions of $\boldsymbol{F}$ and $\boldsymbol{G}_0$, up to and including terms $O(\kappa^2)$, could be obtained entirely from knowledge of the fundamental solution of the quasistatic Stokes equations for an arbitrarily oriented Stokeslet in the tube positioned at O, the latter representing the instantaneous position of, say, the centre of reaction of the moving particle. Evaluation of the requisite velocity dyadics and their gradients necessitates summing an infinite series of infinite integrals (whose integrands entail lengthy arguments of modified Bessel functions). Divergence problems near $\beta = 1$ lead to obvious computational difficulties when the particle centre approaches too closely to the tube wall. Yet the region $\beta \to 1$ is very important hydrodynamically, since wall effects upon the hydrodynamic force and torque are largest in this region.

It has long been established (Happel & Brenner 1965; Hirschfeld 1972; Bungay & Brenner 1973*a*) that as $\beta \to 1$ the values of the material wall tensors for a circular cylinder approach those for a plane wall tangent to the cylinder surface. More precisely, each plane-wall tensor represents the leading term of an asymptotic expansion of its cylinderical counterpart for $|1-\beta| \ll 1$. In this paper we provide the next two higher-order terms in these expansions by employing the regular perturbation scheme initiated by Bungay & Brenner (1973*a*). Calculation of these asymptotic terms involves solving a sequence of half-space Stokes-flow boundary-value problems, satisfying prescribed boundary conditions on a plane wall. The appropriate boundary conditions at a given order of the perturbation scheme derive recursively from knowledge of lower-order perturbation fields in the sequence.

The initial problem of the sequence, which also yields the lowest-order asymptotic term, is that of determining the plane-wall Stokeslet-field velocity dyadic. Beginning with the original work of Lorentz (1896), this problem has been treated in a variety of contexts by Maude (1963), Berker (1963), Wakiya, Darabaner & Mason (1967), Hirschfeld (1972), Aderogba (1977) and Hasimoto & Sano (1980). Subsequent coefficients in the asymptotic expansion derive recursively, as previously indicated. Solution of the necessary Stokes-flow plane-wall boundary-value problems is effected by constructing a representation involving 'Papkovitch–Neuber' potentials (in the manner of Aderogba 1977; Falade 1982), which potentials are then used to obtain the desired particular solutions from the general solution of this class of Stokes-flow problems.

The regular perturbation scheme and resulting sequence of perturbation equations are presented in §2. In §3 we describe the method of solution of these perturbation equations, and calculate from them the ${}_nC_{jk}$ and ${}_nD_{jkl}$ wall-effect tensor coefficients. In the range $0.90 \leqslant \beta \leqslant 0.99$ numerical values furnished by these asymptotic expansions are compared in §4 with the extremely accurate results tabulated by Hirschfeld *et al.* (1984). Excellent agreement is obtained. Generalization to cylinders of other cross-sectional configurations is also briefly discussed in §4, as too is application of the asymptotic analysis to the region *external* to a cylinder.

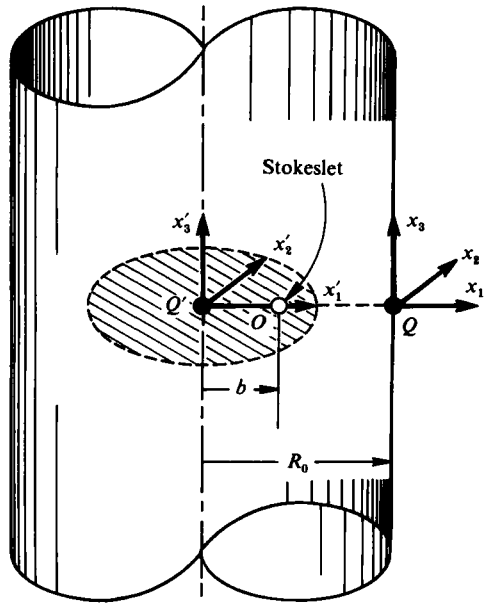

FIGURE 1. Stokeslet singularity O within a circular tube of radius R_0. With (x_1', x_2', x_3') a set of Cartesian axes originating along the tube axis (at Q') the singularity lies at $(b, 0, 0)$. A second set of (dimensionless) Cartesian axes (x_1, x_2, x_3), parallel to the first, originates at the wall (at Q) such that Q', O and Q all lie along the same line. In this non-dimensional system the location of the singularity is at $(-\gamma, 0, 0)$, where the (assumed) small parameter $\gamma = (R_0 - b)/R_0 \ll 1$ represents the fractional distance of the Stokeslet from the wall.

Results presented in this paper are limited to situations in which the particle centre is relatively distant from the wall compared with the particle size – namely $a/(R_0 - b) \ll 1$. Equivalently, $\kappa/(1-\beta) \ll 1$. In contrast, Bungay & Brenner (1973*b*) treat the case of a sphere of radius a for which $\kappa/(1-\beta) = O(1)$ (with $\kappa \ll 1$ and $1-\beta \ll 1$), though in a slightly different physical context from that considered herein. Finally, we note that Tözeren (1982) employs a regular perturbation technique for estimating the torque on a sphere of arbitrary size that is translating and rotating at a slightly off-axis location in the cylinder interior.

2. Formulation

Consider an arbitrarily oriented Stokeslet $\boldsymbol{F}$ positioned at $(b, 0, 0)$ (hereinafter designated as point O) relative to a right-handed Cartesian coordinate system (x_1', x_2', x_3') with origin Q' lying along the axis of a circular cylinder of radius R_0, as in figure 1. Let b and R_0 be such that the ratio $\beta = b/R_0$ is of order unity. Velocity and pressure fields $(\boldsymbol{v}, p)$ at an arbitrary point within the fluid-filled cylinder are assumed to satisfy Stokes' equations

$$\mu \nabla'^2 \boldsymbol{v} - \nabla' p + \boldsymbol{F}\delta'(\boldsymbol{r}') = \boldsymbol{0}, \tag{2.1a}$$

$$\nabla' \cdot \boldsymbol{v} = 0, \tag{2.1b}$$

along with boundary conditions

$$\boldsymbol{v} = \boldsymbol{0} \quad \text{on } x_1'^2 + x_2'^2 = R_0^2 \tag{2.2a}$$

and

$$\boldsymbol{v} \to \boldsymbol{0} \quad \text{as } |x_3'| \to \infty. \tag{2.2b}$$

Here the (dimensional) Dirac delta function $\delta'(\boldsymbol{r}')$ satisfies

$$\int_{V'} \delta'(\boldsymbol{r}')\, \mathrm{d}x_1'\, \mathrm{d}x_2'\, \mathrm{d}x_3' = 1,$$

where region V' includes the Stokeslet. Position vector $\boldsymbol{r}'$ originates at the singularity $(b, 0, 0)$, i.e.

$$|\boldsymbol{r}'| = \{(x_1'-b)^2 + x_2'^2 + x_3'^2\}^{\frac{1}{2}}.$$

In place of the previous coordinate system it is convenient to introduce a stretched non-dimensional right-handed Cartesian coordinate system

$$(x_1, x_2, x_3) = (x_1'-R_0, x_2', x_3')/\gamma R_0 \tag{2.3}$$

(in which $\gamma = 1-\beta$), with origin Q situated at the wall such that Q', O and Q all lie along the same radius vector (see figure 1). In this new coordinate system the Stokeslet is situated at the point $(-1, 0, 0)$. Inasmuch as the original Cartesian system spans the range

$$-R_0 \leqslant x_1' \leqslant R_0, \quad -R_0 \leqslant x_2' \leqslant R_0,$$

along with $-\infty < x_3' < \infty$, the current non-dimensional system spans the range

$$-\frac{2}{\gamma} \leqslant x_1 \leqslant 0, \quad -\frac{1}{\gamma} \leqslant x_2 \leqslant \frac{1}{\gamma}, \tag{2.4}$$

in addition to $-\infty < x_3 < \infty$. Moreover, in the current system the surface of the circular cylinder is described by the *two* branches

$$x_1 = -\{1 \pm (1-\gamma^2 x_2^2)^{\frac{1}{2}}\}/\gamma \tag{2.5}$$

of the generating equation $f(x_1, x_2) = 0$.

In terms of these new coordinates, the original system of equations (2.1) and (2.2) may be rendered parameter-free (except for the parameter γ) by defining dimensionless dyadic 'velocity' and vector 'pressure' fields $(\boldsymbol{V}, \boldsymbol{P})$ such that

$$\boldsymbol{v} = (\gamma R_0 \mu)^{-1}\, \boldsymbol{V}\cdot\boldsymbol{F}, \quad p = (\gamma R_0)^{-2}\, \boldsymbol{P}\cdot\boldsymbol{F}. \tag{2.6a, b}$$

We substitute (2.3) and (2.6) into (2.1) and (2.2) and use the fact that $\boldsymbol{F}$ is an arbitrary vector to obtain the system of dimensionless equations

$$\nabla^2 \boldsymbol{V} - \nabla \boldsymbol{P} + \boldsymbol{I}\delta(\boldsymbol{r}) = \boldsymbol{0}, \tag{2.7a}$$

$$\nabla\cdot\boldsymbol{V} = \boldsymbol{0}, \tag{2.7b}$$

$$\boldsymbol{V} = \boldsymbol{0} \quad \text{on } x_1 = -\{1-(1-\gamma^2 x_2^2)^{\frac{1}{2}}\}/\gamma, \tag{2.8a$_1$}$$

$$\boldsymbol{V} = \boldsymbol{0} \quad \text{on } x_1 = -\{1+(1-\gamma^2 x_2^2)^{\frac{1}{2}}\}/\gamma, \tag{2.8a$_2$}$$

$$\boldsymbol{V} \to \boldsymbol{0} \quad \text{as } |x_3| \to \infty \tag{2.8b}$$

governing the essentially purely geometric fields $(\boldsymbol{V}, \boldsymbol{P})$. Only the scalar parameter γ appears in this system. Here $\boldsymbol{I}$ is the dyadic idemfactor, while $\boldsymbol{r}$ emanates from the singularity $(-1, 0, 0)$; explicitly, $|\boldsymbol{r}| = \{(x_1+1)^2 + x_2^2 + x_3^2\}^{\frac{1}{2}}$. Henceforth all reference to points and surfaces will be made relative to the (x_1, x_2, x_3)-system. Note that the non-dimensional Dirac delta function appearing in (2.7a) is defined such that

$$\int_V \delta(\boldsymbol{r})\, \mathrm{d}x_1\, \mathrm{d}x_2\, \mathrm{d}x_3 = 1,$$

for $\boldsymbol{r}$ included in the volumetric domain V.

2.1. *Perturbation equations*

Equations (2.7)–(2.8) constitute the *exact* system of differential equations and boundary conditions governing the fluid motion created by the presence of the Stokeslet in the tube. What follows is an asymptotic solution for the small-parameter case $\gamma \ll 1$.

2.1.1. *Expansions for* $\boldsymbol{V}$, P

Subject to *a posteriori* verification, we assume the validity of the power-series expansions

$$\boldsymbol{V} = {}_0\boldsymbol{V} + \gamma\, {}_1\boldsymbol{V} + \gamma^2\, {}_2\boldsymbol{V} + \gamma^3\, {}_3\boldsymbol{V} + \ldots, \tag{2.9}$$

and

$$P = {}_0P + \gamma\, {}_1P + \gamma^2\, {}_2P + \gamma^3\, {}_3P + \ldots, \tag{2.10}$$

wherein the perturbation fields $({}_n\boldsymbol{V}, {}_nP)$ $(n = 0, 1, 2, \ldots)$ are each independent of γ.

2.1.2. *Transfer of boundary conditions*

Binomial expansions for small γ of the two branches (2.5) of the equation describing the cylinder wall surface yield respectively

$$x_1 \sim -\tfrac{1}{2}\gamma x_2^2 - \tfrac{1}{8}\gamma^3 x_2^4 - \tfrac{1}{16}\gamma^5 x_2^6 - \tfrac{5}{128}\gamma^7 x_2^8 + \ldots \tag{2.11a}$$

and

$$x_1 \sim -2/\gamma + O(\gamma). \tag{2.11b}$$

In the limit $\gamma \to 0$ the first of these becomes the plane $x_1 = 0$, whereas the second becomes the region $x_1 \to -\infty$ infinitely distant from this plane. In this same limit the domain (2.4) spanned by x_1 and x_2 covers the semi-infinite region $-\infty < x_1 < 0$ and $-\infty < x_2 < \infty$. As a consequence of these facts, in the limit $\gamma \ll 1$ the boundary condition ($2.8a_2$) in conjunction with (2.9) requires that, for $n = 0, 1, 2, \ldots$,

$${}_n\boldsymbol{V} \to \boldsymbol{0} \quad \text{as } x_1 \to -\infty. \tag{2.12a}$$

In addition, the boundary condition ($2.8a_1$) may be transferred to the plane $x_1 = 0$ by expanding $\boldsymbol{V}(x_1, x_2, x_3)$ at the cylinder surface in a Taylor series about $x_1 = 0$ using (2.11*a*). With use of (2.9), this leads to replacement of ($2.8a_1$) by the requirement that (in Cartesian tensor comma notation for derivatives)

$$\begin{aligned}\boldsymbol{0} = {}&{}_0\boldsymbol{V}(0, x_2, x_3) + \gamma[{}_1\boldsymbol{V}(0, x_2, x_3) - \tfrac{1}{2}x_2^2\, {}_0\boldsymbol{V}_{,1}(0, x_2, x_3)] \\ &+ \gamma^2[{}_2\boldsymbol{V}(0, x_2, x_3) - \tfrac{1}{2}x_2^2\, {}_1\boldsymbol{V}_{,1}(0, x_2, x_3) - \tfrac{1}{8}x_2^4\, {}_0\boldsymbol{V}_{,11}(0, x_2, x_3)] \\ &+ \gamma^3[{}_3\boldsymbol{V}(0, x_2, x_3) - \tfrac{1}{2}x_2^2\, {}_2\boldsymbol{V}_{,1}(0, x_2, x_3) - \tfrac{1}{8}x_2^4\, {}_1\boldsymbol{V}_{,11}(0, x_2, x_3) \\ &- \tfrac{1}{48}x_2^6\, {}_0\boldsymbol{V}_{,111}(0, x_2, x_3)] + \ldots .\end{aligned} \tag{2.12b}$$

Equations (2.12*a*, *b*) provide a satisfactory asymptotic approximation of the exact boundary conditions ($2.8a_1$, a_2) for circumstances in which $\gamma = 1 - \beta \ll 1$; that is, where the Stokeslet is very near to the wall compared with the tube radius.

We substitute (2.9), (2.10) and (2.12) into (2.7) and (2.8), collect together terms of like order in γ, and equate to zero each such resulting set of terms. This procedure yields the following sequential sets of differential equations and boundary conditions to be solved in the semi-infinite region $-\infty < x_1 < 0$, $-\infty < x_2 < \infty$, $-\infty < x_3 < \infty$:

zeroth-order equations

$$\nabla^2 {}_0\boldsymbol{V} - \nabla {}_0P + \boldsymbol{I}\delta(\boldsymbol{r}) = \boldsymbol{0}, \quad \nabla \cdot {}_0\boldsymbol{V} = 0, \tag{2.13a, b}$$

$${}_0\boldsymbol{V} = \boldsymbol{0} \quad \text{on } x_1 = 0, \quad {}_0\boldsymbol{V} \to \boldsymbol{0} \quad \text{as } \mathscr{R} \to \infty; \tag{2.14a, b}$$

first-order equations

$$\nabla^2 {}_1\boldsymbol{V} - \nabla {}_1P = \boldsymbol{0}, \quad \nabla \cdot {}_1\boldsymbol{V} = 0, \tag{2.15a, b}$$

$${}_1\boldsymbol{V} = \tfrac{1}{2}x_2^2 {}_0\boldsymbol{V}_{,1} \quad \text{on } x_1 = 0, \quad {}_1\boldsymbol{V} \to \boldsymbol{0} \quad \text{as } \mathscr{R} \to \infty; \tag{2.16a, b}$$

second-order equations

$$\nabla^2 {}_2\boldsymbol{V} - \nabla {}_2P = \boldsymbol{0}, \quad \nabla \cdot {}_2\boldsymbol{V} = 0, \tag{2.17a, b}$$

$${}_2\boldsymbol{V} = \tfrac{1}{2}x_2^2 {}_1\boldsymbol{V}_{,1} + \tfrac{1}{8}x_2^4 {}_0\boldsymbol{V}_{,11} \quad \text{on } x_1 = 0, \quad {}_2\boldsymbol{V} \to \boldsymbol{0} \quad \text{as } \mathscr{R} \to \infty; \tag{2.18a, b}$$

third-order equations

$$\nabla^2 {}_3\boldsymbol{V} - \nabla {}_3P = \boldsymbol{0}, \quad \nabla \cdot {}_3\boldsymbol{V} = 0, \tag{2.19a, b}$$

$${}_3\boldsymbol{V} = \tfrac{1}{2}x_2^2 {}_2\boldsymbol{V}_{,1} + \tfrac{1}{8}x_2^4 {}_1\boldsymbol{V}_{,11} + \tfrac{1}{48}x_2^6 {}_0\boldsymbol{V}_{,111} \quad \text{on } x_1 = 0, \quad {}_3\boldsymbol{V} \to \boldsymbol{0} \quad \text{as } \mathscr{R} \to \infty. \tag{2.20a, b}$$

In the preceding, $\mathscr{R}$ simultaneously denotes both a hemispherical region and its radius, centred at the origin Q of the (x_1, x_2, x_3)-coordinate system, and lying in the semi-infinite region occupied by the fluid. In the limit where the radius $\mathscr{R}$ tends to infinity, and to dominant terms in γ, the origin of this hemispherical region may, when convenient, be chosen to be at the singularity O rather than at Q.

The zeroth-order equations (2.13) and (2.14) may be further delineated into two companion sets. One set defines the fundamental *unbounded* Stokeslet field $({}_0\boldsymbol{V}^0, {}_0\boldsymbol{P}^0)$, satisfying (2.13) and (2.14*b*), but not (2.14*a*). The other defines the 'reflection' $({}_0\boldsymbol{V}^1, {}_0\boldsymbol{P}^1)$ of this fundamental field from the plane $x_1 = 0$ – corresponding to the solution of the system of equations

$$\nabla^2 {}_0\boldsymbol{V}^1 - \nabla {}_0\boldsymbol{P}^1 = \boldsymbol{0}, \quad \nabla \cdot {}_0\boldsymbol{V}^1 = 0, \tag{2.21a, b}$$

$${}_0\boldsymbol{V}^1 = -{}_0\boldsymbol{V}^0 \quad \text{on } x_1 = 0, \quad {}_0\boldsymbol{V}^1 \to \boldsymbol{0} \quad \text{as } \mathscr{R} \to \infty. \tag{2.22a, b}$$

Thus the complete reflected fields $(\boldsymbol{V}_{\mathrm{R}}, \boldsymbol{P}_{\mathrm{R}})$ of the singularity may be expressed as the sums

$$\boldsymbol{V}_{\mathrm{R}} = {}_0\boldsymbol{V}^1 + \gamma\, {}_1\boldsymbol{V} + \gamma^2 {}_2\boldsymbol{V} + \ldots \tag{2.23}$$

and

$$\boldsymbol{P}_{\mathrm{R}} = {}_0\boldsymbol{P}^1 + \gamma\, {}_1\boldsymbol{P} + \gamma^2 {}_2\boldsymbol{P} + \ldots. \tag{2.24}$$

3. Solutions

A general solution of the pair of differential equations

$$\nabla^2 \boldsymbol{V} - \nabla P = \boldsymbol{0}, \quad \nabla \cdot \boldsymbol{V} = 0,$$

in terms of Papkovitch–Neuber potential functions is (Aderogba 1977)

$$2V_{jk} = (\psi_{0k} + x_l \psi_{lk})_{,j} - 2\psi_{jk}, \quad P_k = \psi_{lk,l}, \tag{3.1a, b}$$

in which ψ_{0k} and ψ_{lk} $(k, l = 1, 2, 3)$ are respectively harmonic vector and dyadic fields; that is, each satisfies Laplace's equation. Cartesian tensor fields (V_{jk}, P_k) take their definitions from the relations (summation convention on repeated indices)

$$\boldsymbol{V} = \boldsymbol{i}_j \boldsymbol{i}_k V_{jk}, \quad \boldsymbol{P} = \boldsymbol{i}_k P_k, \tag{3.2a, b}$$

or equivalently

$$V_{jk} = \boldsymbol{i}_k \boldsymbol{i}_j : \boldsymbol{V}, \quad P_k = \boldsymbol{i}_k \cdot \boldsymbol{P}. \tag{3.3a, b}$$

Multiple dot products are to be performed in the order prescribed by the nesting convention (Chapman & Cowling 1970). Here $\boldsymbol{i}_k$ $(k = 1, 2, 3)$ is a unit vector parallel to the x_k direction. Relations similar to (3.2) and (3.3) may be written for the velocity-gradient dyadic and its components, namely

$$\nabla \boldsymbol{V} = \boldsymbol{i}_l \boldsymbol{i}_j \boldsymbol{i}_k V_{jk,l} \quad (V_{jk,l} = \boldsymbol{i}_k \boldsymbol{i}_j (\cdot)^3 \nabla \boldsymbol{V}), \tag{3.4}$$

where $(\cdot)^3$ denotes a triple dot product. To proceed from (3.1) to the unique solutions of (2.15)–(2.22) requires constructing potential functions ψ_{0k} and ψ_{jk} possessing forms necessary for satisfaction of the prescribed boundary conditions. The following theorems prove useful in constructing such potential functions.

(i) If Φ is a biharmonic function, then the function

$$\phi = 2\Phi - x_1 \int \nabla^2 \Phi \, \mathrm{d}x_1 \tag{3.5}$$

is harmonic.

(ii) If ϕ is harmonic then $x_k \phi$ is biharmonic. This together with (3.5) leads to the conclusion that the function

$$\theta = x_k \phi - x_1 \int \phi_{,k} \, \mathrm{d}x_1 \quad (k \neq 1)$$

is also harmonic.

(iii) The biharmonicity of Φ implies the harmonicity of functions X and Y defined (in a hybrid Cartesian-tensor notation) by the relations

$$X = 2x_k \Phi - x_k x_1 \int \nabla^2 \Phi \, \mathrm{d}x_1 - 2x_1 \int \Phi_{,k} \, \mathrm{d}x_1 + x_1^2 \int^2 (\nabla^2 \Phi)_{,k} \, \mathrm{d}x_1 - x_1 \int^3 (\nabla^2 \Phi)_{,k} \, \mathrm{d}x_1,$$

and

$$\begin{aligned} Y = {} & 2x_k^2 \Phi - x_k^2 x_1 \int \nabla^2 \Phi \, \mathrm{d}x_1 - 4x_k x_1 \int \Phi_{,k} \, \mathrm{d}x_1 - 2x_1 \int \Phi \, \mathrm{d}x_1 \\ & + 2x_k x_1^2 \int^2 (\nabla^2 \Phi)_{,k} \, \mathrm{d}x_1 + x_1^2 \int^2 \nabla^2 \Phi \, \mathrm{d}x_1 + 2x_1^2 \int^2 \Phi_{,kk} \, \mathrm{d}x_1 \\ & - 2x_1 x_k \int^3 (\nabla^2 \Phi)_{,k} \, \mathrm{d}x_1 - 2x_1 \int^3 \Phi_{,kk} \, \mathrm{d}x_1 - x_1 \int^3 \nabla^2 \Phi \, \mathrm{d}x_1 \\ & - x_1^3 \int^3 (\nabla^2 \Phi)_{,kk} \, \mathrm{d}x_1 + 3x_1^2 \int^4 (\nabla^2 \Phi)_{,kk} \, \mathrm{d}x_1 - 3x_1 \int^5 (\nabla^2 \Phi)_{,kk} \, \mathrm{d}x_1 \\ & \text{(no sum on } k\text{)}. \end{aligned}$$

Here and throughout the paper, all constants and functions of integration are to be suppressed when evaluating the integrals appearing in these expressions. Notationally, $\int^n ( ) \, \mathrm{d}x_1$ denotes the n-tuple integral with respect to x_1; explicitly,

$$\int^n ( ) \, \mathrm{d}x_1 = \underbrace{\int\int \cdots \int}_{n \text{ times}} ( ) \underbrace{\mathrm{d}x_1 \, \mathrm{d}x_1 \cdots \mathrm{d}x_1}_{n \text{ times}}.$$

The only departure from this convention occurs for the case of a single integral, which retains its customary representation $\int(\,)\,\mathrm{d}x_1$.

(iv) If ϕ is harmonic, so also is

$$Z = x_k^3\phi - 3x_k^2 x_1\int\phi_{,k}\,\mathrm{d}x_1 - 3x_k x_1\int\phi\,\mathrm{d}x_1 + 3x_k x_1^2\int^2\phi_{,kk}\,\mathrm{d}x_1$$
$$+ 3x_1^2\int^2\phi_{,k}\,\mathrm{d}x_1 - 3x_k x_1\int^3\phi_{,kk}\,\mathrm{d}x_1 - 3x_1\int^3\phi_{,k}\,\mathrm{d}x_1$$
$$- x_1^3\int\phi_{,kkk}\,\mathrm{d}x_1 + 3x_1^2\int^4\phi_{,kkk}\,\mathrm{d}x_1 - 3x_1\int^5\phi_{,kkk}\,\mathrm{d}x_1 \quad \text{(no sum on } k\text{)}.$$

The first two of these theorems were enunciated by Aderogba & Chou (1984), while the remaining two may be deduced by the repeated application of the former.

These theorems provide the *Ansatz* for solving (2.13)–(2.22). Solutions for V_{j1}, V_{j2} and V_{j3} will be presented separately. To facilitate comparison of our results with those of Hirschfeld *et al.* (1984), we repeat here the definition of their normalized non-dimensional wall-effect velocity tensors, namely

$${}_jW_{kl} = -6\pi\,{}_jV_{kl}(-1,0,0), \quad {}_jW_{kl,m} = -6\pi\,{}_jV_{kl,m}(-1,0,0).$$

The argument $(-1,0,0)$ denotes evaluation at the Stokeslet position.

3.1. *Solutions for* V_{j1}

3.1.1. *Zeroth-order field of* V_{j1}

The unbounded flow field $({}_0\boldsymbol{V}^0, {}_0P^0)$ generated by a Stokeslet of unit strength located at $(-1,0,0)$ and oriented in the x_1 direction is well known (Happel & Brenner 1965; Aderogba 1977). This field is generated from (3.1) by choosing the potential functions

$$\psi_{01} = \frac{\alpha}{R}, \quad \psi_{j1} = \frac{\delta_{j1}\alpha}{R} \quad (j = 1,2,3), \tag{3.6}$$

with δ_{lm} the Kronecker delta, $R = \{(x_1+1)^2 + x_2^2 + x_3^2\}^{\frac{1}{2}}$ and $\alpha = -(4\pi)^{-1}$. In turn, the reflection (2.21) and (2.22) of this field from the plane $x_1 = 0$ can be obtained by the following choices for ψ_{01} and ψ_{m1}:

$$\psi_{01} = -\frac{\alpha}{R'}, \quad \psi_{j1} = -\delta_{j1}\alpha\left(\frac{1}{R'} + 2R'_{,1}\right), \tag{3.7}$$

where $R' = \{(x_1-1)^2 + x_2^2 + x_3^2\}^{\frac{1}{2}}$.

We substitute (3.7) into (3.1) and evaluate the resulting wall-effect dyadic ${}_0W^1_{j1}$ and its gradient at $(-1,0,0)$ to obtain

$${}_0W^1_{11} = \tfrac{2}{8}, \quad {}_0W^1_{11,1} = \tfrac{2}{16}, \quad {}_0W^1_{21,2} = {}_0W^1_{31,3} = -\tfrac{2}{32}. \tag{3.8}$$

All other components of ${}_0W^1_{j1}$ and ${}_0W^1_{j1,l}$ are zero at $(-1,0,0)$.

On the plane $x_1 = 0$ the combined zeroth-order fields ${}_0\boldsymbol{V} = {}_0\boldsymbol{V}^0 + {}_0\boldsymbol{V}^1$ provide the following velocity-gradient distribution:

$${}_0V_{11,1} = 0, \quad {}_0V_{21,1} = \frac{6x_2\alpha}{\bar{R}^5}, \quad {}_0V_{31,1} = \frac{6x_3\alpha}{\bar{R}^5}, \tag{3.9}$$

where $\bar{R} = (1 + x_2^2 + x_3^2)^{\frac{1}{2}}$.

3.1.2. *First-order field of* V_{j1}

The potential functions satisfying the prescribed boundary conditions

$$ {}_1V_{11} = 0, \quad {}_1V_{21} = \frac{3\alpha x_2^3}{\bar{R}^5}, \quad {}_1V_{31} = \frac{3x_2^2 x_3}{\bar{R}^5} \quad \text{on } x_1 = 0, \tag{3.10} $$

deriving from (2.16*a*) and (3.9) are

$$ \psi_{01} = \psi_{31} = 0, \quad \psi_{21} = \frac{-2\alpha x_2}{R'^3}, \quad \psi_{11} = -\alpha\left[\left\{2\theta_2 - x_1\int\nabla^2\theta_2\,\mathrm{d}x_1\right\}_{,1} + \int\nabla^2\theta_2\,\mathrm{d}x_1\right], \tag{3.11} $$

where

$$ \theta_2 = \frac{x_2^2}{R'^3}. $$

The wall-effect dyadic engendered by (3.11) has as its only non-zero component

$$ {}_1W_{11} = \tfrac{9}{32}. \tag{3.12a} $$

All components of ${}_1W_{j1,l}$ $(j,l = 1,2,3)$ vanish except for the pair†

$$ {}_1W_{21,2} = \tfrac{9}{64}, \quad {}_1W_{31,3} = -\tfrac{9}{64}. \tag{3.12b} $$

Furthermore, evaluation at $x_1 = 0$ yields the velocity dyadic gradients

$$ {}_1V_{11,1} = 3\alpha x_2^2(5\bar{R}^{-7} - \bar{R}^{-5}), \quad {}_1V_{21,1} = 6\alpha x_2(5x_2^2\bar{R}^{-7} - \bar{R}^{-5}), \quad {}_1V_{31,1} = 30\alpha x_2^2 x_3\bar{R}^{-7}. \tag{3.13} $$

3.1.3. *Second-order field of* V_{j1}

We substitute (3.13) and (3.9) into (2.18*a*) to obtain

$$ \left.\begin{aligned} {}_2V_{11} &= -\tfrac{3}{4}\alpha x_2^4(\bar{R}^{-5} + 5\bar{R}^{-7}), \quad {}_2V_{21} = \tfrac{3}{4}\alpha x_2^3(4\bar{R}^{-5} - 15x_2^2\bar{R}^{-7}), \\ {}_2V_{31} &= -\tfrac{45}{4}\alpha x_2^4 x_3\bar{R}^{-5} \end{aligned}\right\} \tag{3.14} $$

on $x_1 = 0$. Appropriate choices of potential functions ensuring satisfaction of (3.14) are

$$ \psi_{01} = \tfrac{3}{4}\alpha\left\{\frac{2x_2^4}{R'^5} - x_2 x_1\int\nabla^2\theta_1\,\mathrm{d}x_1 - 2x_1\int\theta_{1,2}\,\mathrm{d}x_1 + x_1^2\int^2(\nabla^2\theta_1)_{,2}\,\mathrm{d}x_1 - x_1\int^3(\nabla^2\theta_1)_{,2}\,\mathrm{d}x_1\right\}, \tag{3.15a} $$

$$ \psi_{31} = 0, \tag{3.15b} $$

$$ \psi_{21} = -3\alpha\left(2\theta_1 - x_1\int\nabla^2\theta_1\,\mathrm{d}x_1\right), \tag{3.15c} $$

$$ \psi_{11} = -\alpha\left\{-\psi_{01} - 2\psi_{01,1} + \frac{9}{4}\left[2\int\theta_{1,2}\,\mathrm{d}x_1 - x_1\int^2(\nabla^2\theta_1)_{,2}\,\mathrm{d}x_1\right] - \frac{3}{4}\left[x_2\int\nabla^2\theta_1\,\mathrm{d}x_1 - x_1\int^2(\nabla^2\theta_1)_{,2}\,\mathrm{d}x_1\right] + \frac{9}{4}\int^3(\nabla^2\theta_1)_{,2}\,\mathrm{d}x_1\right\}, \tag{3.15d} $$

† In arriving at (3.12) and other similar results, use has been made of the fact that at $(-1,0,0)$

$$ \int^n (R')^{-m}\,\mathrm{d}x_1 = \{(1-m)(2-m)\ldots(n-m)\,2^{n-m}\}^{-1}(-1)^n \quad \text{for } m > n. $$

where $$\theta_1 = \frac{x_2^3}{R'^5}.$$

We substitute (3.15) into (3.1) and evaluate the resulting velocity dyadic and its gradient at $(-1,0,0)$. This yields

$$ {}_2W_{11} = \tfrac{27}{256}, \quad {}_2W_{11,1} = -\tfrac{27}{512}, \quad {}_2W_{21,2} = \tfrac{51}{1024}, \quad {}_2W_{31,3} = -\tfrac{99}{1024}. \tag{3.16}$$

All other components of ${}_2W_{j1}$ and ${}_2W_{j1,l}$ are zero.

3.2. *Solutions for* V_{j2}

3.2.1. *Zeroth-order field of* V_{j2}

The fundamental field ${}_0V^0_{j2}$ created by a Stokeslet at $(-1,0,0)$ oriented in the x_2 direction has as its generating potential functions

$$\psi_{02} = 0, \quad \psi_{j2} = \frac{\delta_{j2}\alpha}{R}. \tag{3.17}$$

The reflection of this field from the plane $x_1 = 0$ is described by the potential functions

$$\psi_{02} = \psi_{32} = 0, \quad \psi_{12} = \frac{-2\alpha x_2}{R'^3}, \quad \psi_{22} = \frac{-\alpha}{R'}. \tag{3.18}$$

Tensor constants W_{j2} and $W_{j2,k}$ $(j,k = 1,2,3)$ associated with the reflected field have as their only non-zero components

$$ {}_0W^1_{22} = \tfrac{9}{16}, \quad {}_0W^1_{12,2} = {}_0W^1_{22,1} = \tfrac{9}{32}. \tag{3.19}$$

On $x_1 = 0$ the combined zeroth-order field gives the following velocity-gradient distribution for ${}_0V_{j2,1}$:

$$ {}_0V_{12,1} = 0, \quad {}_0V_{22,1} = 6\alpha x_2^2 \bar{R}^{-5}, \quad {}_0V_{32,1} = 6\alpha x_2 x_3 \bar{R}^{-5}. \tag{3.20}$$

3.2.2. *First-order field of* V_{j2}

The algebraic detail required to calculate this first-order perturbation field (as well as the subsequent second-order field of V_{j2}), though straightforward in principle, proved quite tedious in execution. Indeed, the calculations were virtually an order of magnitude less tractable, and the resulting algebraic formulas concomitantly more unwieldy, than those required for the more symmetrical (indeed axisymmetrical) fields V_{j1}, for which the Stokeslet was oriented normal to the wall. To avoid presenting these excessively long formulas, we will therefore suppress all algebraic detail, proceeding directly to a summary of the final results obtained.

After establishing that $\psi_{32} = 0$, and obtaining the non-zero expressions for the remaining potential functions $\psi_{\lambda 2}$ $(\lambda = 0,1,2)$ satisfying the requisite boundary conditions, it was found that at $(-1,0,0)$ the only non-zero components of ${}_1W_{j2}$ and ${}_1W_{j2,l}$ were respectively

$$ {}_1W_{22} = \tfrac{81}{128} \quad \text{and} \quad {}_1W_{12,2} = \tfrac{27}{64}. \tag{3.21}$$

3.2.3. *Second-order field of* V_{j2}

Again, $\psi_{32} = 0$ was the only potential function of the four $\psi_{\lambda 2}$ that was eliminated from further consideration. This eventually resulted in the following non-zero components of ${}_2W_{j2}$ and ${}_2W_{j2,l}$ at $(-1,0,0)$:

$$ {}_2W_{22} = \tfrac{477}{512}, \quad {}_2W_{22,1} = -\tfrac{441}{1024}, \quad {}_2W_{12,2} = \tfrac{63}{1024}. \tag{3.22}$$

3.3. *Solutions for* V_{j3}

3.3.1. *Zeroth-order field of* V_{j3}

Using (3.1), the fundamental field ${}_0V^0_{j3}$ of an unbounded Stokeslet situated at $(-1,0,0)$ and oriented in the x_3 direction admits the potential functions

$$\psi_{03} = 0, \quad \psi_{j3} = \frac{\delta_{j2}\alpha}{R}. \tag{3.23}$$

In turn, the reflection of this field from the plane $x_1 = 0$ is the field arising from the potential functions

$$\psi_{03} = \psi_{23} = 0, \quad \psi_{13} = \frac{-2\alpha x_3}{R'^3}, \quad \psi_{33} = \frac{-\alpha}{R'}. \tag{3.24}$$

Resulting non-zero components of the wall-effect dyadic at $(-1,0,0)$ engendered by (3.24) and its gradients are

$${}_0W^1_{33} = \tfrac{9}{16}, \quad {}_0W^1_{13,3} = {}_0W^1_{33,1} = \tfrac{9}{32}. \tag{3.25}$$

On $x_1 = 0$ the velocity-gradient distribution ${}_0V_{j2,1}$ of the combined zeroth order fields is

$${}_0V_{13,1} = 0, \quad {}_0V_{23,1} = 6\alpha x_2 x_3 \bar{R}^{-5}, \quad {}_0V_{33,1} = 6\alpha x_3^2 \bar{R}^{-5}. \tag{3.26}$$

3.3.2. *First-order field of* V_{j3}

Here again, all algebraic details will be suppressed in the interests of brevity. All of the $\psi_{\lambda 3}$ ($\lambda = 0,1,2,3$ are here required to satisfy the boundary conditions required of ${}_1V_{13}, {}_1V_{23}$ and ${}_1V_{33}$. At $(-1,0,0)$ the wall-effect dyadic and its gradient are found to possess the following non-zero components:

$${}_1W_{33} = \tfrac{27}{128}, \quad {}_1W_{13,3} = \tfrac{9}{64}, \tag{3.27}$$

all other components being zero.

3.3.3. *Second-order field of* V_{j3}

The boundary conditions demanded of ${}_2V_{j3}$ require all four potential functions $\psi_{\lambda 3}$. Resulting non-zero wall-effect coefficients eventually obtained upon evaluation at $(-1,0,0)$ are

$${}_2W_{33} = \tfrac{153}{512}, \quad {}_2W_{13,3} = \tfrac{99}{1024}, \quad {}_2W_{33,1} = -\tfrac{81}{512}. \tag{3.28}$$

4. Results and discussion

It follows from the results of §3 that the wall-effect tensors W_{jk} and $W_{jk,l}$ of Hirschfeld *et al.* (1984) can be expressed asymptotically, either in the respective forms

$$W_{jk} = {}_0C_{jk}\gamma^{-1} + {}_1C_{jk} + {}_2C_{jk}\gamma + O(\gamma^2) \tag{4.1}$$

and

$$W_{jk,l} = {}_0D_{jkl}\gamma^{-2} + {}_1D_{jkl}\gamma^{-1} + {}_2D_{jkl} + O(\gamma), \tag{4.2}$$

or, since $\gamma = 1-\beta$, in the equivalent forms cited in the Abstract. Coefficients ${}_nC_{jk}$ and ${}_nD_{jkl}$ ($n = 0,1,2$) are tabulated as the rational fractions appearing in tables 1 and 2 respectively. Coefficients failing to appear explicitly in these tables are identically zero.

Tables 1 and 2 have been used to compute values of the non-zero components of W_{jk} and $W_{jk,l}$ in the range $0.90 \leqslant \beta \leqslant 0.99$. These approximate asymptotic values

jk \ n	${}_nC_{jk}$		
	0	1	2
11	$\frac{9}{8}$	$\frac{9}{32}$	$\frac{27}{256}$
22	$\frac{9}{16}$	$\frac{81}{128}$	$\frac{477}{512}$
33	$\frac{9}{16}$	$\frac{27}{128}$	$\frac{153}{512}$†

† Preliminary announcements (Hirschfeld *et al.* 1984; Brenner 1984) of present results incorrectly give the ${}_2C_{33}$ coefficient as $\frac{77}{256}$, rather than as the correct value of $\frac{153}{512}$ here tabulated.

TABLE 1. Coefficients ${}_nC_{jk}$ for use in (4.1) from $n = 0, \ldots, 2$. For $j \neq k$, ${}_nC_{jk} = 0$.

jkl \ n	${}_nD_{jkl}$		
	0	1	2
111	$\frac{9}{16}$	0	$-\frac{27}{512}$
212	$-\frac{9}{32}$	$\frac{9}{64}$	$\frac{153}{1024}$
221	$\frac{9}{32}$	0	$-\frac{441}{1024}$
122	$\frac{9}{32}$	$\frac{27}{64}$	$\frac{63}{1024}$
133	$\frac{9}{32}$	$\frac{9}{64}$	$\frac{99}{1024}$
313	$-\frac{9}{32}$	$-\frac{9}{64}$	$-\frac{99}{1024}$
331	$\frac{9}{32}$	0	$-\frac{81}{512}$

TABLE 2. Coefficients ${}_nD_{jkl}$ for use in (4.2) from $n = 0, \ldots, 2$. All components of ${}_nD_{jkl}$ that do not appear explicitly are zero-valued.

are compared in table 3 with the 'exact' numerical values tabulated by Hirschfeld *et al.*, the latter of which are believed to be correct to the last significant figure shown. Agreement is quite good, especially at those β-values closest to unity. Further improvement in accuracy of the asymptotic wall-effect values would require computation of higher-order terms in n – an algebraically very tedious and lengthy exercise.

Hirschfeld *et al.* demonstrated that the wall-effect tensors possess the properties

$$W_{jk,j} = 0 \tag{4.3}$$

and

$$W_{jk,3} = -W_{kj,3}. \tag{4.4}$$

These relations are obviously consistent with the individual coefficient values explicitly and implicitly tabulated in tables 1 and 2, and separately consistent for each n-value of ${}_nC_{jk}$ and ${}_nD_{jkl}$.

4.1. *The region external to a cylinder*

The utility of knowledge of W_{jk} and $W_{jk,l}$ versus β in calculating wall effects to $O(\kappa^2)$ in the *interior* of a circular cylinder has been thoroughly discussed by Hirschfeld *et al.* (1984). Additionally, it should be mentioned that (4.1) and (4.2) – together with the coefficients tabulated in tables 1 and 2 – simultaneously provide the appropriate Stokeslet wall-effect tensors for a particle located in the infinite fluid-filled space *external* to a solid circular cylinder, provided that γ $(= 1-\beta)$ is replaced by $-\gamma$ $(= \beta-1)$ in (4.1) and (4.2), and that the ${}_nD_{jkl}$ values for the external case are taken to be opposite in algebraic sign from those tabulated in table 2. This appears to be the first instance in which such 'exterior' wall effects have been addressed.

(*a*)

	W_{11}		W_{22}		W_{33}	
β	asymptotic approximation (4.1)	'exact' value	asymptotic approximation (4.1)	'exact' value	asymptotic approximation (4.1)	'exact' value
9.90	11.5418	11.5419	6.351	6.343	5.87	5.91
0.91	12.79074	12.79080	6.967	6.961	6.49	6.52
0.92	14.35219	14.35224	7.739	7.734	7.27	7.30
0.93	16.36006	16.36008	8.734	8.730	8.27	8.29
0.94	19.03758	19.03759	10.064	10.061	9.60	9.62
0.95	22.786523	22.786530	11.929	11.927	11.476	11.488
0.96	28.410469	28.410471	14.733	14.731	14.285	14.293
0.97	37.784414	37.784415	19.4107	19.4100	18.969	18.974
0.98	56.533359	56.533360	28.7764	28.7761	28.3419	28.3441
0.99	112.78230	112.78232	56.8921	56.8920	56.4639	56.4645

(*b*)

	$W_{11,1}$		$W_{21,2}$		$W_{22,1}$	
β	asymptotic approximation (4.2)	'exact' value	asymptotic approximation (4.2)	'exact' value	asymptotic approximation (4.2)	'exact' value
0.90	56.1972	56.1957	−26.569	−26.567	27.69	27.72
0.91	69.3917	69.3905	−33.010	−33.008	34.29	34.32
0.92	87.8379	87.8370	−42.038	−42.036	43.514	43.534
0.93	114.7432	114.7426	−55.240	−55.237	56.967	56.982
0.94	156.1973	156.1969	−75.632	−75.630	77.694	77.703
0.95	224.9473	224.9470	−109.5381	−109.5364	112.069	112.072
0.96	351.50976	351.50964	−172.1162	−172.1148	175.351	175.347
0.97	624.94726	624.94721	−307.6631	−307.6620	312.07	312.06
0.98	1406.1973	1406.1973	−695.9443	−695.9436	702.69	702.68
0.99	5624.9472	5624.9491	−2798.2881	−2798.2899	2812.07	2812.04

	$W_{12,2}$		$W_{13,3} = -W_{31,3}$		$W_{33,1}$	
β	asymptotic approximation (4.2)	'exact' value	asymptotic approximation (4.2)	'exact' value	asymptotic approximation (4.2)	'exact' value
0.90	32.41	32.34	29.6279	29.6291	28.0	27.6
0.91	39.47	39.41	36.3814	36.3828	34.5	34.2
0.92	49.28	49.23	45.7998	45.8013	43.8	43.5
0.93	63.49	63.44	59.5036	59.5051	57.2	56.9
0.94	85.22	85.18	80.5654	80.5670	78.0	77.7
0.95	121.00	120.97	115.4092	115.4106	112.34	112.12
0.96	186.39	186.36	179.3934	179.3498	175.62	175.43
0.97	326.62	326.60	317.2842	317.2852	312.34	312.20
0.98	724.280	724.267	710.2529	710.2536	702.97	702.87
0.99	2854.749	2854.743	2826.6592	2826.6593	2812.34	2812.29

TABLE 3. Comparison of asymptotic values derived (*a*) from (4.1) and (*b*) from (4.2) with 'exact' values taken from Hirschfeld *et al.* (1984) in the range $0.90 \leqslant \beta \leqslant 0.99$.

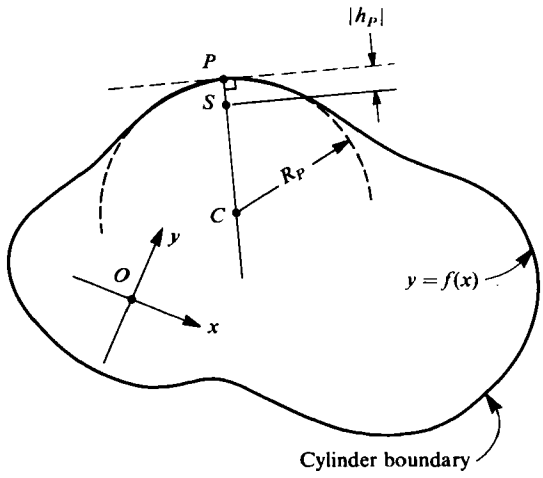

FIGURE 2. Stokeslet singularity S near the boundary of a non-circular cylinder.

4.2. *Non-circular cylinders*

Minor modifications permit the present scheme to be adapted to the case of asymptotic wall effects for cylinders of *non-circular* cross-section. In this context we consider the cylinder whose cross-section in the plane $z = \text{const}$ is bounded by the generator

$$y = f(x), \tag{4.5}$$

where f is some analytic function. Here (x, y, z) denote a rectangular system of (dimensional) Cartesian coordinates with origin at O in figure 2. It will be assumed henceforth that the cylinder boundary (4.5) is closed, though easily achieved circumstances exist in which the subsequent theory remains valid even if this is not the case.

Let $S \equiv (x_S, y_S)$ (with $z_S = 0$) denote the position of the Stokeslet, and $P \equiv (x_P, y_P)$ that point on the boundary (4.5) lying nearest to S. Specifically, x_P is that value of x (within the domain of variation of x over the curve (4.5)) that minimizes the distance function

$$|h(x)| = \{(x-x_S)^2 + [f(x)-y_S]^2\}^{\frac{1}{2}}; \tag{4.6}$$

that is, for a prescribed S and cylinder-generating function $f(x)$,

$$|h(x_P)| = |h_P|, \text{ say, } = \min |h(x)|. \tag{4.7}$$

Corresponding to this value of x_P is the magnitude

$$|h_P| = \{(x_P-x_S)^2 + [f(x_P)-y_S]^2\}^{\frac{1}{2}} \tag{4.8}$$

of the distance of the Stokeslet from the cylinder wall. (Subsequently we will assign an algebraic sign to h_P.) Naturally, as indicated in figure 2, the line segment SP intersects the boundary curve (4.5) orthogonally.

Provided that $f''(x_P) \neq 0$, the magnitude R_P of the local radius of curvature of the cylinder at P is given by the well-known expression

$$R_P = \frac{\{1+[f'(x_P)]^2\}^{\frac{3}{2}}}{|f''(x_P)|}. \tag{4.9}$$

This radius will always be taken to be a non-negative-definite quantity. The centre of curvature $C \equiv (x_C, y_C)$ is situated at the point

$$x_C = x_P + (x_S - x_P)\gamma^{-1}, \tag{4.10a}$$

$$y_C = y_P + (y_S - y_P)\gamma^{-1}, \tag{4.10b}$$

where γ is the algebraically signed scalar

$$\gamma = \frac{h_P}{R_P} \quad (|\gamma| \ll 1). \tag{4.11}$$

Point C lies on the concave side of the generator at P. In figure 2, points P, S and C all lie along the same straight line. Our implicit convention regarding the algebraically signed scalar h_P is that $h_P > 0$ when S in figure 2 lies on the concave side of the generator at P, and conversely; that is, h_P is respectively positive or negative according as the Stokeslet is 'internal' or 'external' to the cylinder.

It will prove convenient to simultaneously rotate, translate and non-dimensionalize the (x, y)-coordinate system to produce a new Cartesian system (x_1, x_2) defined by the linear transformation

$$-x_1 = \frac{(x-x_P)(x_S-x_P)+(y-y_P)(y_S-y_P)}{(x_S-x_P)^2+(y_S-y_P)^2}, \tag{4.12a}$$

$$-x_2 = \frac{(x-x_P)(y_S-y_P)-(y-y_P)(x_S-x_P)}{(x_S-x_P)^2+(y_S-y_P)^2}. \tag{4.12b}$$

(The denominator of each of the above terms is h_P^2. They are here written out explicitly so that subsequent cancellation with comparable terms arising in the numerators will be evident.) Locations of pertinent points in the (x_1, x_2)-system are as follows:

$$P \equiv (0,0), \quad S \equiv (-1,0), \quad C \equiv (-\gamma^{-1}, 0). \tag{4.13}$$

In this Cartesian system the locations of P, S and C are now the same as for the circular-cylinder (x_1, x_2)-case in §2. Indeed, it was to achieve precisely this equivalence that motivated the coordinate transformation (4.12).

In this dimensionless Cartesian system the equation of the circle of curvature that is tangent to the generating curve at P and is centred at C is

$$(x_1-\gamma^{-1})^2+x_2^2 = \gamma^{-2}, \tag{4.14}$$

exactly as in the case of the circular cylinder (cf. (2.5)). As follows from the definition of the circle of curvature, to terms of lowest orders in γ the local portion of the cylinder-generator curve (4.5) immediately proximate to P necessarily coincides with the small-$|\gamma|$ series expansion of (4.14); that is, the cylinder surface is locally described to terms of the first order in γ by the equation (cf. (2.11*a*))

$$x_1 \sim -\tfrac{1}{2}\gamma x_2^2 + O(\gamma^2), \tag{4.15}$$

exactly as in the circular-cylinder case.

Since the fluid-velocity field is required to satisfy the boundary condition $\boldsymbol{v} = \boldsymbol{0}$ on the surface (4.5), it follows immediately from our prior analysis of the comparable circular-cylinder case that the zeroth- and first-order wall-effect tensors ${}_0\boldsymbol{W}$ and ${}_1\boldsymbol{W}$

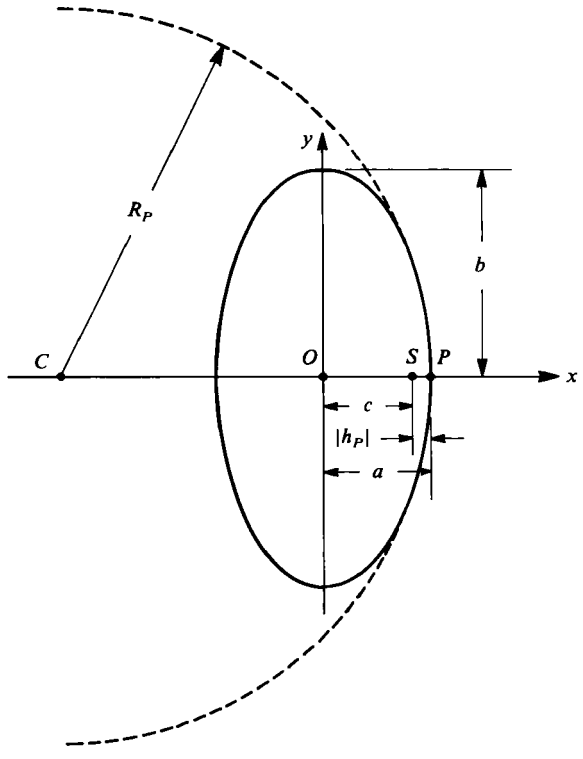

FIGURE 3. Stokeslet singularity S near the boundary of an elliptic cylinder of semiaxes a and b.

for the non-circular-cylinder case are given quite generally by precisely the same formulas as for the circular cylinder; explicitly (cf. (4.1)),

$$W_{jk} = {}_0C_{jk}\gamma^{-1} + {}_1C_{jk} + O(\gamma) \tag{4.16}$$

and

$$W_{jk,l} = {}_0D_{jkl}\gamma^{-2} + {}_1D_{jkl}\gamma^{-1} + O(1). \tag{4.17}$$

Here γ is given for the non-circular case by (4.11), whereas the required four numerical tensors ${}_0C_{jk}, \ldots, {}_1D_{jkl}$ are those given in tables 1 and 2 (cf. the remarks at the end of §4.1 when $\gamma < 0$, i.e. when the Stokeslet S shown in figure 2 lies instead on the convex side of the curve at P, corresponding to wall effects when the Stokeslet lies in the region *external* to the non-circular cylinder). Calculation of the higher-order wall-effect tensor ${}_2\boldsymbol{W}$ in the preceding expression, though straightforward in principle, would call for extraordinary algebraic effort involving taking account of the 'curvature of the curvature'.

The non-dimensional wall-effect formulas (4.16) and (4.17) permit immediate calculation (Hirschfeld *et al.* 1984) of the Stokes force $\boldsymbol{F}$ and torque $\boldsymbol{G}_S$ on a particle moving in close proximity to a non-circular cylindrical boundary. In using the Hirschfeld *et al.* formulas for $\boldsymbol{F}$ and $\boldsymbol{G}_S$, it is necessary to use our radius of curvature R_P in place of their circular-cylindrical radius R_0.

By way of example, we consider the elliptic cylinder (figure 3)

$$\left(\frac{x}{a}\right)^2 + \left(\frac{y}{b}\right)^2 = 1, \tag{4.18}$$

corresponding to the functional dependence

$$f(x) = \pm\left(\frac{b}{a}\right)(a^2-x^2)^{\frac{1}{2}} \tag{4.19}$$

in (4.5). For definiteness the Stokeslet will be supposed to lie along the x-axis at the point $(x_S, y_S) = (c, 0)$ with $c > 0$,† and such that

$$|a-c|/a \ll 1; \tag{4.20}$$

the latter assures proximity of the Stokeslet to the wall. Moreover, again for definiteness, it will be further supposed that

$$a/b \leqslant 1. \tag{4.21}$$

In the present example (4.6) becomes

$$h^2(x) = (x-c)^2 + \left(\frac{b}{a}\right)^2(a^2-x^2).$$

Since points x lying on the boundary of the ellipse span the region $-a \leqslant x \leqslant a$, and given the inequality (4.21), the function $|h(x)|$ attains its minimum value at the endpoint $x = a$. Hence $(x_P, y_P) = (a, 0)$, whence, from (4.8), $h_P = a-c$ – the algebraic sign having been chosen in accord with our concave/convex convention for the Stokeslet location. Straightforward calculation via (4.9) of the radius of curvature at P gives $R_P = b^2/a$. (In view of the assumed inequality (4.21), this makes $R_P \geqslant b \geqslant a$, with equality holding only for the circular-cylindrical case $a = b$. Thus, as shown in figure 3, R_P exceeds both b and a in magnitude.)‡ Hence, from (4.11),

$$\gamma = \left(\frac{a}{b}\right)^2\frac{a-c}{a}, \tag{4.22}$$

for the elliptic-cylinder case. Given the inequalities (4.20) and (4.21), it is indeed true in present circumstances that $|\gamma| \ll 1$. Use of (4.22) in (4.16) and (4.17) furnishes the lower-order wall-effect tensors for both the internal and external elliptic-cylinder cases.

This work was begun while A. F. was on sabbatical leave from the University of Lagos. He is grateful to the latter for support as well as to MIT for providing a hospitable environment during his stay there.

REFERENCES

ADEROGBA, K. 1977 On eigenstresses in dissimilar media. *Phil. Mag.* A **35**, 281–292.

ADEROGBA, K. & CHOU, T.-W. 1984 The generation of generalized prepotential functions and related problems. *Proc. R. Soc. Lond.* (in press).

BERKER, R. 1963 Intégration des équations du mouvement d'un fluide visqueux incompressible. In *Handbuch der Physik, vol.* VIII/2: *Fluid Dynamics II* (ed. S. Flügge & C. Truesdell), pp. 242–244. Springer.

† Although figure 3 as drawn shows the *internal*-Stokeslet case ($c < a$), our analysis applies equally well to the *external*-Stokeslet case ($c > a$).

‡ For completeness, we note from (4.10) that the centre of curvature is located at the point

$$x_C = -\frac{b^2-a^2}{a}, \quad y_C = 0$$

lying to the left of the origin in figure 3.

BRENNER, H. 1984 Antisymmetric stresses induced by the rigid-body rotation of dipolar suspensions: vortex flows. *Intl J. Engng Sci.* **22**, 645–682.

BUNGAY, P. M. & BRENNER, H. 1973*a* Pressure drop due to the motion of a sphere in proximity to a wall bounding a Poiseuille flow. *J. Fluid Mech.* **60**, 81–96.

BUNGAY, P. M. & BRENNER, H. 1973*b* The motion of a closely-fitting sphere in a fluid-filled tube. *Intl J. Multiphase Flow* **1**, 25–56.

CHAPMAN, S. & COWLING, T. G. 1970 *The Mathematical Theory of Non-Uniform Gases*, 3rd edn. Cambridge University Press.

COX, R. G. & BRENNER, H. 1967 Effect of finite boundaries on the Stokes resistance of an arbitrary particle. Part 3. Translation and rotation. *J. Fluid Mech.* **28**, 391–411.

FALADE, A. 1982 Arbitrary motion of an elliptic disc at a fluid interface. *Int. J. Multiphase Flow* **8**, 543–551.

HAPPEL, J. & BRENNER, H. 1965 *Low Reynolds Number Hydrodynamics*. Prentice-Hall.

HASIMOTO, H. & SANO, O. 1980 Stokeslets and eddies in creeping flow. *Ann. Rev. Fluid Mech.* **12**, 335–363.

HIRSCHFELD, B. R. 1972 A theoretical study of the slow asymmetric settling of an arbitrarily positioned particle in a circular cylinder. Ph.D. dissertation, New York University.

HIRSCHFELD, B. R., BRENNER, H. & FALADE, A. 1984 First- and second-order wall effects upon the slow viscous asymmetric motion of an arbitrarily-shaped, -positioned and -oriented particle within a circular cylinder. *PhysicoChem. Hydrodyn.* **5**, 99–133.

LORENTZ, H. A. 1896 A general theorem concerning the motion of a viscous fluid with some applications. *Zittingsverlag Akad. Wet. Amsterdam* **5**, 168–175; see also *Abhandlungen über theoretische Physik* Bd. 1, S. 23–42, Leipzig 1907.

MAUDE, A. D. 1963 The movement of a sphere in front of a plane at low Reynolds number. *Brit. J. Appl. Phys.* **14**, 894–898.

TÖZEREN, H. 1982 Torque on eccentric spheres flowing in tubes. *Trans. ASME* E: *J. Appl. Mech.* **49**, 279–283.

WAKIYA, S., DARABANER, C. L. & MASON, S. G. 1967 Particle motions in sheared suspensions. XXI: interactions of rigid spheres. *Rheol. Acta* **6**, 264–273.